HETEROCLINIC DYNAMICS AND ATTITUDE MOTION CHAOTIZATION OF COAXIAL BODIES AND DUAL-SPIN SPACECRAFT

Anton V. Doroshin*
S.P. Korolev Samara State Aerospace University (National Research University), Samara, Russia.

Abstract. Heteroclinic dynamics of a free coaxial bodies system and dual-spin spacecraft is examined. New analytical solutions for heteroclinic orbits, corresponded to the polhodes-separatrices in the space of the angular moment components, are obtained. On the base of these analytical heteroclinic solutions analysis of possibility of the system motion chaotization with the help of Melnikov method is conducted. The analysis shows the polhode-separatrix-orbit splitting at presence of small harmonical perturbation torques between the coaxial bodies. The separatrix splitting generates the chaotic layer near the unperturbed separatrix region. This fact proves possibility of realization of non-regular dynamics and chaotic tilting motion of the dual-spin spacecraft.

Keywords: Coaxial Bodies; Dual-Spin Spacecraft; Attitude Motion; Heteroclinic Orbit; Heteroclinic Analytical Solutions; Melnikov Method; Motion Chaotization; Tilting Motion; Poincaré Sections.

MSC2010: 70E17, 34C28, 37D45

Introduction

Analysis and synthesis of attitude motion of gyrostat-satellites and dual-spin spacecraft (DSSC) still remain very important research area of modern spaceflight dynamics. Non-linear motion modes, attitude control, stabilization of spatial orientation and reorientation process of spinning spacecraft and gyrostat-satellites are being examined by many authors. This topic connected with classical problems of rotating motion of rigid body, gyrostat and coaxial bodies systems. Furthermore, it offers quite models, dynamical systems and research methods in the field of non-linear dynamics.

Classical results of rigid body and gyrostats angular (rotational) motion investigation have been collected in many treatises, for example, in [1, 2]. Important aspects of rigid body dynamics were presented in [3-6]. Some aspects of gyrostat free motion dynamics in Andoyer–Deprit phase space were studied in [7].

Papers [8, 9, 10] gave a description of motion of dual-spin spacecraft at realization of a momentum transfer maneuver with rotor-body spinup. This maneuver realization can demonstrate motion evolutions with nontrivial change of attitude orientation and spacecraft longitudinal axis tumble. These evolutions were explained with the help of direct analysis of motion equations, numerical experiments and on the base of probabilistic analysis of separatrix crossing [8]. Dynamics analysis of modes motion of variable mass (structure) coaxial bodies and dual-spin spacecraft with time-dependent inertia moments was conducted, for example, in [11, 18].

Recently, research topics of many authors have been focussed on non-linear and chaotic phenomena into rotating motion dynamics of rigid body, gyrostat and coaxial system. Non-integrable cases, non-regular and chaotic modes of coaxial bodies and gyrostat motion and theirs applications to the spaceflight mechanics tasks were considered in [6-21].

One of the powerful analytical techniques of analysis of dynamical systems chaotization is the Melnikov method [22]. The Melnikov method is an effective analytical tool to determine the splitting and multiple intersections of homo/heteroclinic orbit. With the use of the Melnikov method, several studies were conducted on the chaotic dynamics of the rigid body, gyrostat, coaxial bodies and DSSC [11-16, 21 and others], including local chaotization investigation on

* Correspondence to: A.V. Doroshin, Samara State Aerospace University, SSAU, Moscovskoe shosse 34, Samara, Russia 443086. E-mail: doran@inbox.ru.

the base of higher-dimensional expansions of the Melnikov method, which had been developed by Wiggins [23], Holmes and Marsden [24].

The splitting of polhodes-separatrices-orbits implies separation and multiple intersections of stable and unstable manifolds of saddle heteroclinic points, which limit the heteroclinic orbit. Therefore close to the perturbed heteroclinic orbit phase trajectory forms very complicated heteroclinic net [25], which generates the chaotic layer near the unperturbed separatrix region. Inside the chaotic layer phase trajectory can passes through different phase space regions and, therefore, it performs complicated evolution with repeated escapes (rotation-oscillation-rotation-…). This fact has proved possibility of realization of non-regular dynamics and complex tilting motion of dual-spin spacecraft.

On purpose to apply the Melnikov method for analysis of the DSSC perturbed motion chaotization we have obtained in this paper new analytical heteroclinic solutions for angular velocity components of the coaxial bodies system, which consists of a body-carrier and a body-rotor. These solutions, corresponded to heteroclinic orbits (polhodes) on the inertia ellipsoid of the carrier, are the main necessary element for proof of heteroclinic polhode-separatrix-orbit splitting at presence of small harmonical perturbation torques on the base of Melnikov method. Here we can note, that in [24] analysis of attitude motion chaotization of the coaxial bodies system (as rigid body with rotor-attachment) have been conducted on the base of classical analytical solutions for the heteroclinic orbits of free *single* rigid body (in the absence of native heteroclinic solutions, corresponded to the coaxial bodies system).

Task of heteroclinic solutions obtaining in similar formulation was considered in [1, 2, 12 and 16]. In contrast to [1, 12] in this paper native dynamics of the coaxial bodies investigates, without maintaining of constancy of gyrostatic moment (also called as relative angular moment of rotor(s) in carrier body frame: $h_z = C_1\sigma \neq \text{const}$).

In Ref. [16] heteroclinic solutions were obtained in the Andoyer–Deprit canonical variables on the base of classical procedure [for example, 26] for integration of a second order differential equations system (for single degree-of-freedom system), which include following four main steps: 1) the system first integral (energy integral/ Hamiltonian) identification, 2) use of the first integral to reduction of the second order system to the first order system, 3) integration of the first order differential equation in explicit form (in quadrature), 4) inversion of the quadrature and reduction to obtain the single-valued final solution. This procedure was effective applied by prof. Aslanov to obtaining of the coaxial bodies heteroclinic solutions in Ref. [16]. With the help of Ref. [16] solutions heteroclinic dependencies for the coaxial bodies angular velocity components can be written, but in this case shape of solutions will be cumbersome: expressions will include compositions of radicals, exponents, trigonometric functions and inverse trigonometric functions at the same time.

In Ref. [12] important closed-form of the heteroclinic solutions for gyrostat with constant gyrostatic moments $\left(h_x, h_y, h_z - \text{const}\right)$ were obtained with the help of Volterra-Wangerin-Wittenburg method. Analytical solutions for angular velocity components of the body-carrier [12] in this case have cumbersome shape with fractional polynomial functions of hyperbolic tangents (highest power of polynomials equal to 12). Practical use of solutions of Ref. [12] involves great difficulties at analytical and numerical computations.

Thus, in present paper on the base of Euler dynamical equations we have obtain new simple form of the heteroclinic solutions for the coaxial bodies system in the space of angular velocity components.

In addition to powerful analytical examination, it is very important to provide a many-sided numerical analysis of chaotic modes in the system. Thereupon, in this article we have use effective numerical tools such as construction of time-dependencies graphs, perturbed polhodes 3D-curves, Poincaré sections, plotting of heteroclinic net as a set of Poincaré map images of unperturbed separatrix polhode and corresponded invariant fractal set (Smale's horseshoes) in neighborhood of the unperturbed separatrix.

Also we note that some other methods and models of non-linear dynamics systems theory may be applied to research of chaotization of the system motion. First of all, detection and identification of irregular attractors (strange/chaotic/quasi) of different type (Lorenz, Ressler, Newton-Leipnik, Sprott, etc.) in the three-dimensional space of angular velocity components can be implemented [20, 26]. Non-regular modes also can be illustrated [20] with the help of 1) construction of complex power spectra of fast Fourier transformation, 2) plotting of compound hodograph of coaxial system longitudinal axis vector, 3) calculation of positive Lyapunov exponents. Widespread (global) chaos in the system can be shown on the base of Chirikov method of overlapping resonances [26, 27] and Greene method of individual system invariant tori breakdown [26, 28].

The present paper is organized as follows. In section 1 the mathematical model of the coaxial bodies system and DSSC perturbed attitude motion is constructed. In section 2 the explicit analytical solutions for the heteroclinic separatrices orbits in the space of the angular moment components are obtained. In section 3 local chaotization of the motion is conducted on the base of Melnikov method at presence of small harmonic torque of the coaxial bodies internal interaction. In section 4 chaotic motion numerical modeling results are presented.

1. The motion equation of the coaxial bodies and DSSC

Let us consider free attitude motion of the coaxial bodies and DSSC (body #1 is rotor; body #2 is main/core/carrier body). Assume that the carrier body has triaxial inertia tensor and the rotor is dynamically symmetrical body. We introduce the following systems of coordinates (Fig.1): *OXYZ* is the inertial system of coordinates, $Ox_2y_2z_2$ – the connected principal system of coordinates of the carrier body, and $Ox_1y_1z_1$ – the connected principal system of coordinates of the rotor body. The Oz_1 and Oz_2 axes of the connected systems are identical to the common rotation axis of the coaxial bodies.

The system motion is described on the base of Euler dynamical equations [1, 2, 8, 11, 18, 19, 20], and with the help of Andoyer–Deprit canonical variables [3, 4, 7, 12, 16]. The dynamical Euler equation of free motion of the coaxial system with four degree of freedom can be written as [18]:

$$\begin{cases} A\dot{p} + \left(C - B\right)qr + qC_1\sigma = 0, \\ B\dot{q} + \left(A - C\right)pr - pC_1\sigma = 0, \\ C\dot{r} + C_1\dot{\sigma} + \left(B - A\right)pq = 0, \\ C_1\left(\dot{r} + \dot{\sigma}\right) = M_\Delta, \end{cases} \tag{1.1}$$

or in the following form:

$$\begin{aligned} &A\dot{p} + \left(C_2 - B\right)qr + q\Delta = 0, \qquad B\dot{q} + \left(A - C_2\right)pr - p\Delta = 0, \\ &C_2\dot{r} + \dot{\Delta} + \left(B - A\right)pq = 0, \qquad \dot{\Delta} = M_\Delta, \end{aligned} \tag{1.2}$$

where $\{p,q,r\}$ are components of the carrier body angular velocity which represented in projections onto axes of the $Ox_2y_2z_2$ frame; $\sigma -$ the rotor angular velocity relative the carrier body; $\mathbf{I}_2 = diag\left[A_2, B_2, C_2\right]$ is the triaxial inertia tensors of the carrier body in the connected frame $Ox_2y_2z_2$; $\mathbf{I}_1 = diag\left[A_1, A_1, C_1\right]$ is the inertia tensors of the dynamically symmetrical rotor in the connected frame $Ox_1y_1z_1$; $A = A_1 + A_2$, $B = A_1 + B_2$, $C = C_1 + C_2$ are the main inertia moments of the coaxial bodies system in the frame $Ox_2y_2z_2$ (including rotor); $M_\Delta -$ is the internal torque of the coaxial bodies interaction; $\Delta = C_1\left(r+\sigma\right) -$ the longitudinal angular moment of the rotor along Oz_1; $C_1\sigma = h_{z_1}$ – the rotor relative angular moment in the carrier body frame $Ox_2y_2z_2$. Assume that $A_2 > B_2 > C_2 > A_1 > C_1$.

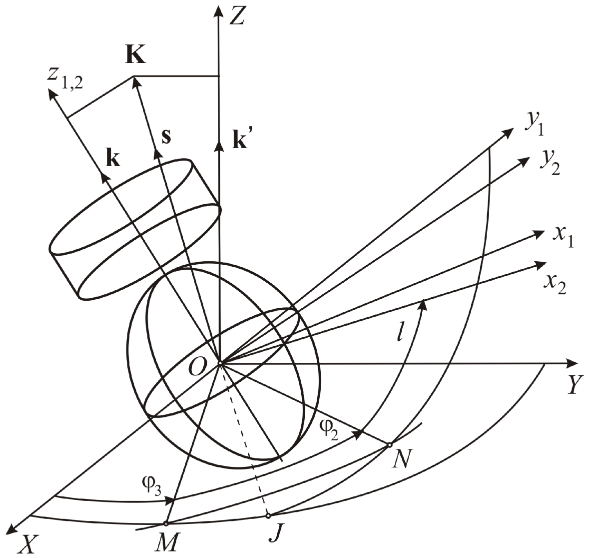

Fig.1. *The coaxial bodies system and the coordinate frames*

Here we note that the equation system (1.1) corresponded to the free motion of the coaxial bodies and the unbalanced gyrostat with non-constant rotor relative angular moment $h_{z_1} = C_1\sigma \neq \text{const}$ (even if $M_\Delta = 0$). In this case analysis results for balanced $(h = \text{const})$ gyrostat [1, 2, 12] are not applicable.

In the following research we will use also the Hamilton form of equations in the Andoyer–Deprit canonical variables. The Andoyer–Deprit variables [3, 4] can be expressed with the help of the coaxial system angular moment **K** (fig.1):

$$L = \frac{\partial T}{\partial \dot{l}} = \mathbf{K}\cdot\mathbf{k};\ I_2 = \frac{\partial T}{\partial \dot{\varphi}_2} = \mathbf{K}\cdot\mathbf{s} = |\mathbf{K}| = K;\ I_3 = \frac{\partial T}{\partial \dot{\varphi}_3} = \mathbf{K}\cdot\mathbf{k}';\quad L \le I_2$$

$$K_{x_2} = Ap = \sqrt{I_2^2 - L^2}\sin l;\ K_{y_2} = Bq = \sqrt{I_2^2 - L^2}\cos l;\ K_{z_2} = C_2 r + \Delta = L. \tag{1.3}$$

In the Andoyer–Deprit variables the system Hamiltonian takes the form:

$$H = H_0 + \varepsilon H_1;\quad H_0 = T = \frac{I_2^2 - L^2}{2}\left[\frac{\sin^2 l}{A_1 + A_2} + \frac{\cos^2 l}{A_1 + B_2}\right] + \frac{1}{2}\left[\frac{\Delta^2}{C_1} + \frac{(L-\Delta)^2}{C_2}\right], \tag{1.4}$$

where T – system kinetic energy; ε – small non-dimensional parameter; H_1 is perturbed part of the Hamiltonian.

As is follows from the Hamiltonian (1.4), I_2, I_3 and φ_3 are constants in unperturbed case. Then corresponded dynamical system has one degree of freedom $\{l, L\}$:

$$\begin{gathered} \dot{L} = f_L(l,L) + \varepsilon g_L(t); \qquad \dot{l} = f_l(l,L) + \varepsilon g_l(t) \\ f_L(l,L) = -\frac{\partial H_0}{\partial l} = \alpha\left(I_2^2 - L^2\right)\sin l\cos l \\ f_l(l,L) = \frac{\partial H_0}{\partial L} = L\left[\frac{1}{C_2} - \frac{\sin^2 l}{(A_1 + A_2)} - \frac{\cos^2 l}{(A_1 + B_2)}\right] - \frac{\Delta}{C_2} \\ g_L = -\frac{\partial H_1}{\partial l};\quad g_l = \frac{\partial H_1}{\partial L} \end{gathered} \tag{1.5}$$

where $\alpha = \left(A_1 + B_2\right)^{-1} - \left(A_1 + A_2\right)^{-1}$.

We consider the coaxial system perturbed motion in the case when the DSSC rotor spinup [9, 10] already was finished, and the rotor was taken the constant angular velocity and the corresponded constant longitudinal angular moment $\bar{\Delta} = \text{const}$. Assume that small $(\mu << 1)$ disturbance harmonic internal torque takes place [21]:

$$M_\Delta = \mu \cos \nu t \tag{1.6}$$

The torque (1.6) describes, for example, a signal of control system of internal spinup engine (the rotor angular velocity stabilization system) at presence of latency of angular velocity sensor.

From the last equation (1.2) at presence of the small torque (1.6) the analytical solution follows

$$\Delta(t) = \bar{\Delta} + (\mu / \nu)\sin \nu t$$

In this case we get the system (1.5) with the perturbations

$$g_L\left(t\right) = 0; \quad g_l\left(t\right) = -\nu \sin \nu t \tag{1.7}$$

and with the small non-dimensional parameter

$$\varepsilon = \frac{\mu}{\nu^2 C_2} \tag{1.8}$$

In the next section on purpose to apply the Melnikov method for analysis of the DSSC perturbed motion chaotization we will obtain new analytical heteroclinic solutions for angular velocity components of the coaxial bodies system.

2. Explicit analytical heteroclinic solutions in the space of the angular moment components

Let us obtain the analytical solution for the heteroclinic orbit in the space of angular moment components.

Theorem 1. *Assume the coaxial bodies interaction absence $\left(M_\Delta = 0\right)$. Then the following heteroclinic solutions $\left\{\bar{p}\left(t\right), \bar{q}\left(t\right), \bar{r}\left(t\right)\right\}$ of the system* (1.2) *for the free coaxial bodies take place:*

$$\bar{p}\left(t\right) = \pm\sqrt{\frac{C_2\left(B - C_2\right)}{A\left(A - B\right)}}\,y\left(t\right); \quad \bar{q}\left(t\right) = \pm\sqrt{s^2 - k^2\left(y\left(t\right) + \Delta\beta\right)^2}; \quad \bar{r}\left(t\right) = y\left(t\right) + \frac{\Delta}{B - C_2};$$

$$y\left(t\right) = \frac{4a_0 E\left(y_0^\pm\right)\exp\left(\mp\dfrac{M\sqrt{a_0}}{k^2}t\right)}{\left[E\left(y_0^\pm\right)\exp\left(\mp\dfrac{Mt\sqrt{a_0}}{k^2}\right) - a_1\right]^2 - 4a_2 a_0}, \tag{2.1}$$

with the set of constants, which depend on only inertia parameters and initial condition of motion:

$$\Delta = \text{const} > 0;\; a_2 = -k^2;\; a_1 = -2\Delta\beta k^2;\; a_0 = s^2 - k^2\Delta^2\beta^2;\; y_0^\pm = \pm\frac{s}{k} - \Delta\beta;\; \beta = \left(B - C_2\right)^{-1} - \left(A - C_2\right)^{-1};$$

$$s^2 = \frac{H}{B\left(A - B\right)};\quad k^2 = \frac{C_2\left(A - C_2\right)}{B\left(A - B\right)};\quad H = 2T\left(A - \tilde{D}\right) + \Delta^2 b;\quad \tilde{D} = \frac{\Delta^2 a}{2T} + B;\quad T = \textit{kinetic energy level};$$

$$M = \frac{\left(A - C_2\right)}{B}\sqrt{\frac{C_2\left(B - C_2\right)}{A\left(A - B\right)}};\qquad a = \frac{C_1 C_2 + \left(B - C_2\right)\left(C_1 - B\right)}{\left(B - C_2\right)C_1};\qquad b = \frac{C_2 C_1 + \left(A - C_2\right)\left(C_1 - A\right)}{\left(A - C_2\right)C_1}.$$

Examination and the theorem proof.

First of all we define the term "polhode". The polhode [1] is a curved line of intersection of the body angular velocity vector with the body inertia ellipsoid surface. Also the polhode is the fourth-order curve of intersection of a kinetic energy ellipsoid and an angular moment ellipsoid, which are defined with the help of following expression:

$$Ap^2 + Bq^2 + C_2 r^2 + \frac{\Delta^2}{C_1} = 2T \tag{2.2}$$

$$A^2 p^2 + B^2 q^2 + \left[C_2 r + \Delta\right]^2 = K^2 = 2DT \tag{2.3}$$

$$D = \frac{K^2}{2T} \tag{2.4}$$

Parameter D [1] can change magnitude in some interval, and each value D defines the concrete polhode with corresponded values of the system kinetic energy and the system angular moment. Full set of D values defines full set of the polhodes. Thus, we can obtain the set of the polhodes on the base of

a) the kinetic energy ellipsoid and its intersection with the set of ellipsoids of the angular moment,

b) the angular moment ellipsoid and its intersection with the set of ellipsoids of the kinetic energy.

In any case, the polhode is the parametrized curve $\{p(t), q(t), r(t)\}$ in the space $\mathbb{R}^3 : (p, q, r)$.

Projections and general view of the angular moment ellipsoid with the polhodes are indicated in Figure 2. On the ellipsoid four different areas take place [1, 5, 7, 11]. These areas are divided by the separatrices-polhodes, which represent the heteroclinic orbits "saddle-to-saddle" in the phase space of the angular velocity components. These orbits form "big ellipses" (thick lines in fig.2).

It is needed to note, that position of the separatrices-polhodes depend on Δ value. If Δ value increases then the separatrices-polhodes move along the axis Or with rise of distance $O\tilde{O}$. At critical value [16] $\Delta = \Delta^* = K(B - C_2)/B$ point $\tilde{O}$ move to vertex of the ellipsoid, as indicated in Figure 3. In this case three areas of polhodes remain in the ellipsoid surface, and the separatrices-polhodes become tangential "big ellipses" (instead of intersecting "big ellipses" in fig.2) [7, 11, 16]. If $\Delta^* < \Delta < \Delta^{**} = K(A - C_2)/A$ then topology of polhodes on the ellipsoid remains "critical" structure (fig.3), but the "big ellipses" become "big drops" [7, 11, 16] (fig.4-a). If $\Delta = \Delta^{**}$ then "big drops" collapse – in this case ellipsoid has one-areas-topology (fig.4-b).

We can write polhodes equations [1] on the base of combination of expressions (2.2) and (2.3). Multiplication (2.2) by A and deduction (2.3) give us

$$B(A-B)q^2 + C_2(A-C_2)r^2 + C_1(A-C_1)(r+\sigma)^2 - 2C_1C_2 r(r+\sigma) = 2T(A-D) \tag{2.5}$$

Multiplication (2.2) by C_1 and deduction (2.3) give us

$$A(C_1 - A)p^2 + B(C_1 - B)q^2 + C_2(C_1 - C_2)r^2 - 2C_1C_2 r(r+\sigma) = 2T(C_1 - D) \tag{2.6}$$

Multiplication (2.2) by B and deduction (2.3) give us

$$A(B-A)p^2 + B\left(C_2 r^2 + C_1[r+\sigma]^2\right) - \left(C_2 r + C_1[r+\sigma]\right)^2 = 2T(B-D) \tag{2.7}$$

Expressions (2.5) and (2.6) can be rewritten as follows

$$0 \le B(A-B)q^2 + C_2(A-C_2)r^2 + C_1(A-C_1)(r+\sigma)^2 = 2T(A-D) + 2C_1C_2 r(r+\sigma)$$

$$0 \le A(A-C_1)p^2 + B(B-C_1)q^2 + C_2(C_2-C_1)r^2 = -2T(C_1-D) - 2C_1C_2 r(r+\sigma)$$

From last formulas the boundary conditions for D value follow

$$C_1 + C_1C_2 r\left(r+\sigma\right)/T \le D \le A + C_1C_2 r\left(r+\sigma\right)/T$$

Formula (2.7) is the q-independent expression which defines the polhodes equation on the coordinate plane Opr (fig.2). We can rewrite (2.7) take in to account perfect square

$$-A\left(A-B\right)p^2 + C_2\left(B-C_2\right)\left[r-\frac{\Delta}{B-C_2}\right]^2 = F \tag{2.8}$$

where $\qquad F = 2T\left(B-D\right)+\Delta^2 a, \qquad a = \dfrac{C_1C_2+\left(B-C_2\right)\left(C_1-B\right)}{\left(B-C_2\right)C_1}$

We introduce the shifted coordinate axes $\tilde{O}p\tilde{r}$ (fig.2) and scalable component of the angular velocity

$$\tilde{r} = r - \frac{\Delta}{B-C_2} \tag{2.9}$$

From (2.8) the canonical form of equation of hyperbolas follows, which correspond to the polhodes in the plane $\tilde{O}p\tilde{r}$

$$-A\left(A-B\right)p^2 + C_2\left(B-C_2\right)\tilde{r}^2 = F \tag{2.10}$$

If F=0 then from equation (2.10) we obtain dependencies for asymptotes of the hyperbolas (straight line equations):

$$\sqrt{A\left(A-B\right)}p = \pm\sqrt{C_2\left(B-C_2\right)}\tilde{r} \tag{2.11}$$

The relation

$$F = 0 \tag{2.12}$$

defines connection between initial conditions of realization of motion along hyperbolas asymptotes. We can consider (2.12) as equation for value D

$$F = 2T\left(B-D\right)+\Delta^2 a = 0 \quad \Rightarrow \quad \tilde{D} = \frac{\Delta^2 a}{2T} + B \tag{2.13}$$

So, equality $D = \tilde{D}$ is the condition of realization of motion along hyperbolas asymptotes ($\tilde{D}$ is the root of (2.12)).

Assume that $q(t=0) = q_0 = 0$ (or assume that initial time-moment t=0 correspond to moment when the q-component equal to zero). Then equation (2.12) can be considered as quadratic equation

$$2TB - K^2 + \Delta^2 a = 0 \quad \Rightarrow \quad \left(Ap_0^2 + C_2 r_0^2 + \Delta^2/C_1\right)B - A^2p_0^2 + \left[C_2 r_0 + \Delta\right]^2 + \Delta^2 a = 0 \tag{2.14}$$

We can find value r_0 as the root of (2.14) at arbitrary values p_0 and Δ

$$r_0 = r_0^{(1,2)} = f\left(p_0, \Delta\right) \tag{2.15}$$

From expression (2.5), take into account perfect square, follow

$$B\left(A-B\right)q^2 + C_2\left(A-C_2\right)\left[r-\frac{\Delta}{A-C_2}\right]^2 = 2T\left(A-D\right)+\Delta^2 b \tag{2.16}$$

$$b = \frac{C_2C_1+\left(A-C_2\right)\left(C_1-A\right)}{\left(A-C_2\right)C_1}$$

We can consider (2.16) as equation of ellipses on the coordinate plane Oqr (fig.2). Substitution $D = \tilde{D}$ into (2.16) give us equation for the "big ellipses", corresponded to the projections of the separatrices-polhodes:

$$B\left(A-B\right)q^2 + C_2\left(A-C_2\right)\tilde{\tilde{r}}^2 = H \tag{2.17}$$

where $H = 2T\left(A-\tilde{D}\right)+\Delta^2 b$.

It is needed to note, that the canonical ellipse equation (2.17) is written in the shifted axes $\tilde{\tilde{O}}\tilde{\tilde{q}}\tilde{\tilde{r}}$, where scalable component of the angular velocity is used

$$\tilde{\tilde{r}} = r - \frac{\Delta}{A - C_2} \tag{2.18}$$

Thus, we have two equations (2.11) and (2.17), which define the second-order curves, corresponded to two projections of the three-dimensional separatrix-polhode.

Let us obtain exact explicit analytical solution for the heteroclinic separatrix orbits with the help of the second Euler equation (1.2), expressions (2.11) and (2.17). Equation (2.11) can be rewritten as

$$p = \pm\sqrt{\frac{C_2\left(B - C_2\right)}{A\left(A - B\right)}}\left[\tilde{\tilde{r}} - \Delta\beta\right] \tag{2.19}$$

where $\beta = \left(B - C_2\right)^{-1} - \left(A - C_2\right)^{-1}$.

From (2.17) follow

$$\tilde{\tilde{r}}^2 = \frac{s^2 - q^2}{k^2} \tag{2.20}$$

$$s^2 = \frac{H}{B\left(A - B\right)} = \text{const}; \quad k^2 = \frac{C_2\left(A - C_2\right)}{B\left(A - B\right)} = \text{const}$$

On the base of (2.20) and (2.19) we can rewrite the second equation (1.2) in the form

$$B\dot{q} \pm \left(A - C_2\right)\sqrt{\frac{s^2 - q^2}{k^2}}\sqrt{\frac{C_2\left(B - C_2\right)}{A\left(A - B\right)}}\left[\pm\sqrt{\frac{s^2 - q^2}{k^2}} - \Delta\beta\right] = 0 \tag{2.21}$$

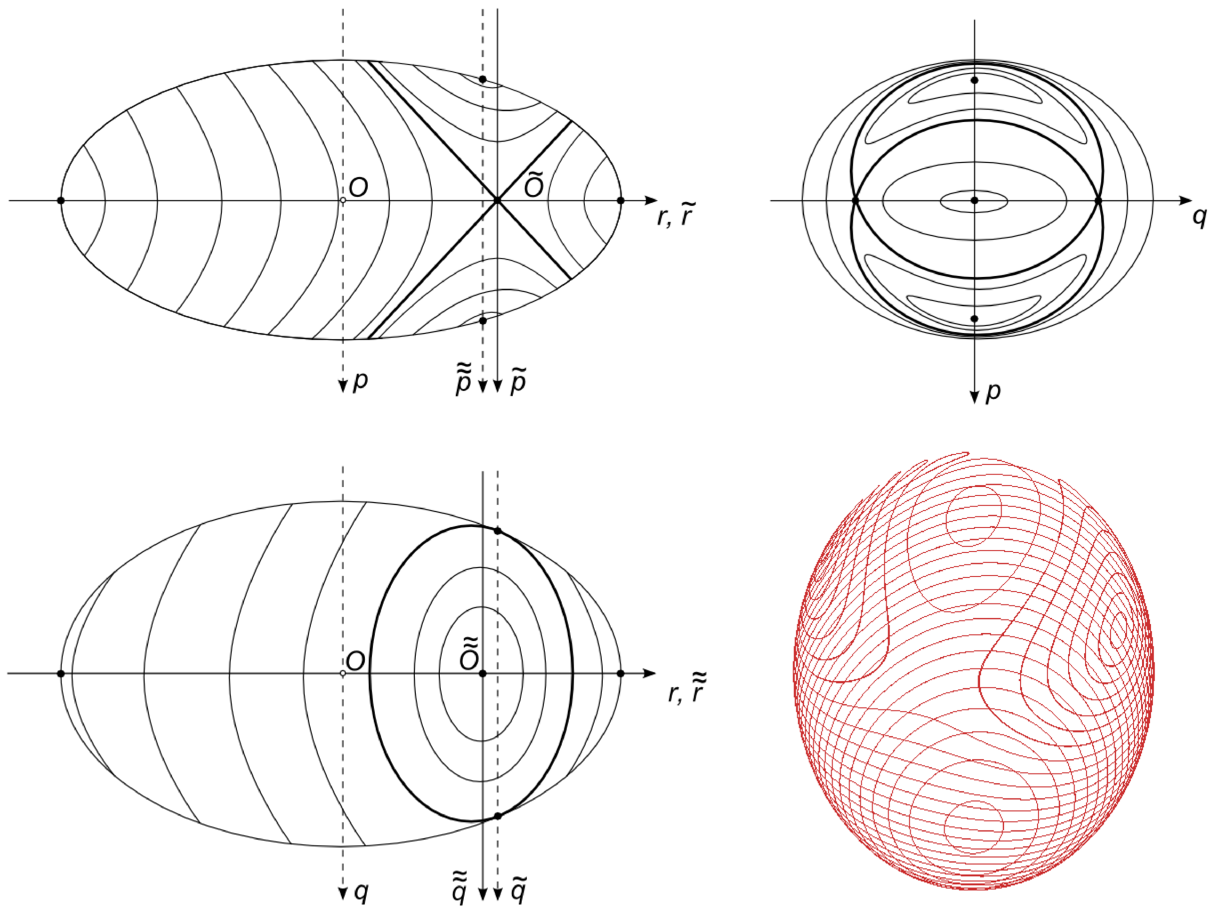

Fig.2

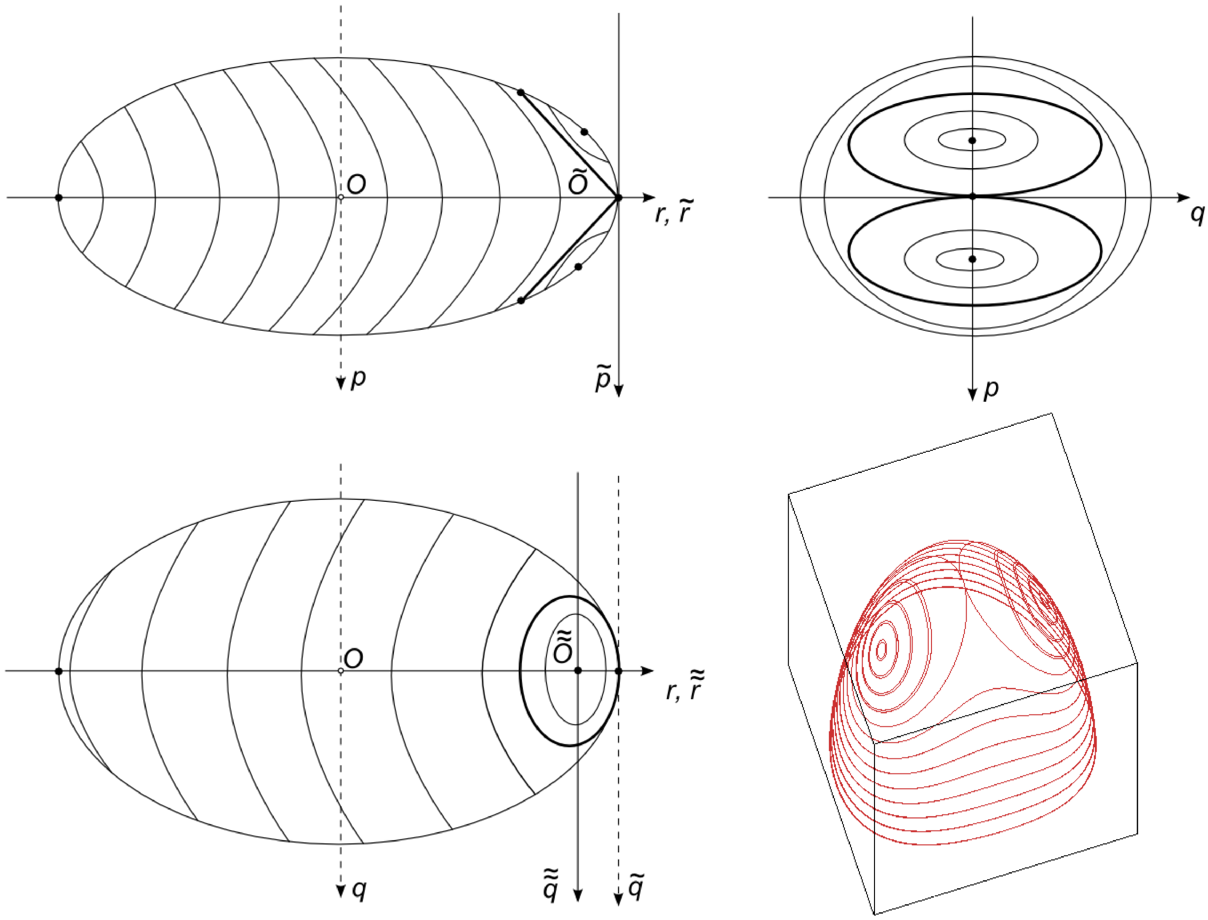
O
$\tilde{O}$
$r, \tilde{r}$
p
$\tilde{p}$
q
p
O
$\tilde{\tilde{O}}$
$r, \tilde{\tilde{r}}$
q
$\tilde{\tilde{q}}$
$\tilde{q}$

Fig.3

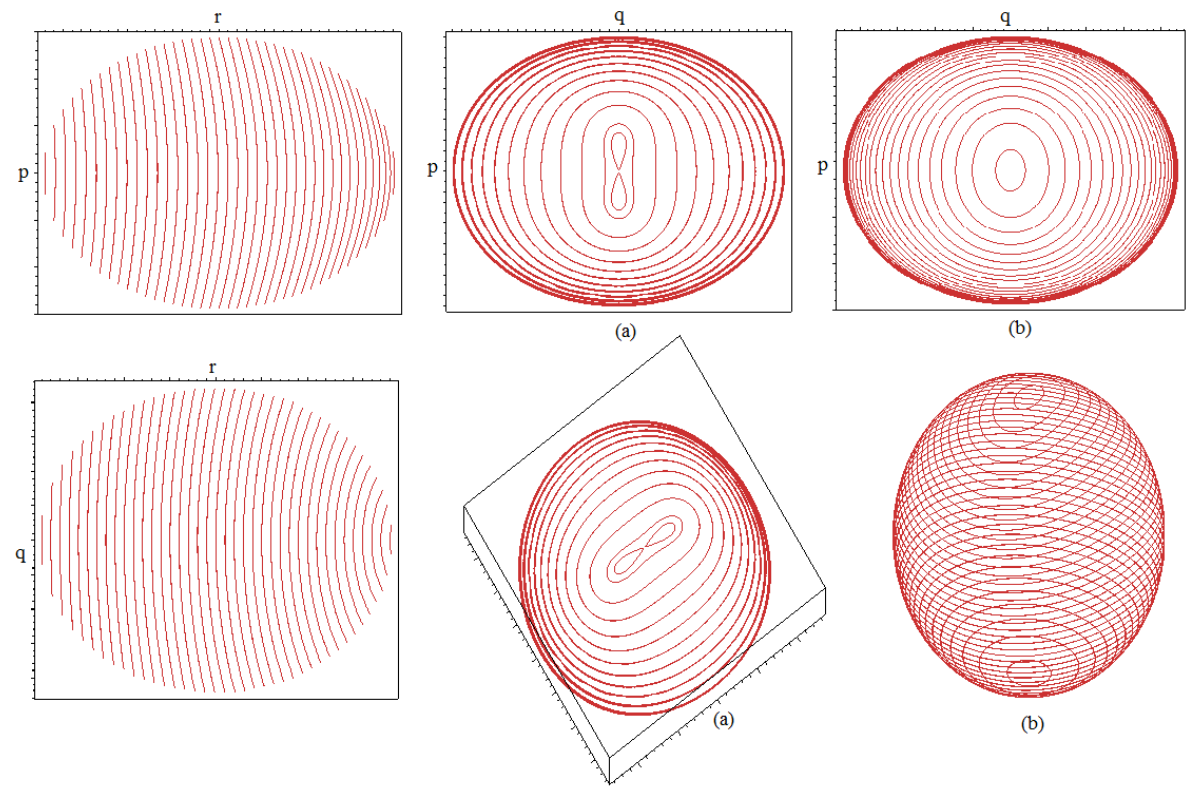
r
p
q
p
(a)
q
p
(b)
r
q
(a)
(b)

Fig.4

The differential equation (2.21) contains possible quaternary signs alternation, corresponded to the four heteroclinic orbits "saddle-to-saddle". These four orbits form the "big ellipses".

We make the change of variable

$$x=\sqrt{\frac{s^2-q^2}{k^2}} \tag{2.22}$$

From (2.22) follow

$$q=\pm\sqrt{s^2-k^2x^2}; \qquad dq=\frac{\mp k^2 x dx}{\sqrt{s^2-k^2x^2}}$$

Then equation (2.21) is rewritten in differential form

$$\begin{gathered}\frac{k^2 dx}{[\pm x-\Delta\beta]\sqrt{s^2-k^2x^2}}=\pm M dt\\ M=\frac{(A-C_2)}{B}\sqrt{\frac{C_2(B-C_2)}{A(A-B)}}\end{gathered} \tag{2.23}$$

Equation (2.23) includes two cases of signs of the x-variable. In the both cases we make corresponded substitutions

$$1).\ \left[\begin{array}{l}\dfrac{k^2 dx}{[x-\Delta\beta]\sqrt{s^2-k^2x^2}}=\pm M dt\\ y=x-\Delta\beta\\ x=y+\Delta\beta;\quad dx=dy\\ y_0=x_0-\Delta\beta\\ \dfrac{k^2 dy}{y\sqrt{s^2-k^2x^2}}=\pm M dt\end{array}\right. \qquad 2).\ \left[\begin{array}{l}\dfrac{k^2 dx}{[-x-\Delta\beta]\sqrt{s^2-k^2x^2}}=\pm M dt\\ y=-x-\Delta\beta\\ x=-y-\Delta\beta;\quad dx=-dy\\ y_0=-x_0-\Delta\beta\\ \dfrac{-k^2 dy}{y\sqrt{s^2-k^2x^2}}=\pm M dt\end{array}\right. \tag{2.24}$$

As we can see from the last expressions (2.24), both cases give interconnected equation again

$$\frac{k^2 dy}{y\sqrt{s^2-k^2x^2}}=\pm M dt \tag{2.25}$$

Take into account twoness of the initial condition $\left(y_0=\pm x_0-\Delta\beta\right)$ from (2.25) follow

$$\int_{y_0}^{y}\frac{dy}{y\sqrt{s^2-k^2\left(y^2+2\Delta\beta y+\Delta^2\beta^2\right)}}=\frac{\pm Mt}{k^2};\quad y_0=y_0^{\pm}=\pm x_0-\Delta\beta;\quad x_0=\frac{s}{k} \tag{2.26}$$

Expression (2.26) reduces to the standard integral [29]

$$\begin{gathered}\int_{y_0}^{y}\frac{dy}{y\sqrt{s^2-k^2\left(y^2+2\Delta\beta y+\Delta^2\beta^2\right)}}=\int_{y_0}^{y}\frac{dy}{y\sqrt{a_2y^2+a_1y+a_0}}=\mathbb{F}(y)-\mathbb{F}\left(y_0^{\pm}\right)\\ a_2=-k^2;\quad a_1=-2\Delta\beta k^2;\quad a_0=s^2-k^2\Delta^2\beta^2\end{gathered} \tag{2.27}$$

where antiderivative $\mathbb{F}(y)$ has the following shape

$$\mathbb{F}(z)=\frac{-1}{\sqrt{a_0}}\ln E(z);\quad E(z)=\frac{2a_0+a_1z+2\sqrt{a_0}\sqrt{a_2z^2+a_1z+a_0}}{z};\quad a_0>0$$

From (2.27) we get the solution of equation (2.25)

$$E(y(t))=E\left(y_0^{\pm}\right)\exp\left(\mp\frac{M\sqrt{a_0}}{k^2}t\right) \tag{2.28}$$

After transformations the exact explicit analytical solution for the time-dependence $y(t)$ follows

$$y(t)=\frac{4a_0E\left(y_0^{\pm}\right)\exp\left(\mp\dfrac{M\sqrt{a_0}}{k^2}t\right)}{\left[E\left(y_0^{\pm}\right)\exp\left(\mp\dfrac{Mt\sqrt{a_0}}{k^2}\right)-a_1\right]^2-4a_2a_0}\qquad(2.29)$$

It is needed to note, that the quadrature (2.27) is quite frequent for heteroclinic solutions in rigid body dynamics [15, 16].

Making back substitutions we get the exact explicit analytical heteroclinic solutions for all components of the angular velocity of carrier body – $\left\{\bar{p}(t),\bar{q}(t),\bar{r}(t)\right\}$:

$$\begin{cases}\bar{p}(t)=\pm\sqrt{\dfrac{C_2\left(B-C_2\right)}{A\left(A-B\right)}}y(t)\\ \bar{q}(t)=\pm\sqrt{s^2-k^2\left(y(t)+\Delta\beta\right)^2}\\ \bar{r}(t)=y(t)+\dfrac{\Delta}{B-C_2}\end{cases}\qquad(2.30)$$

So, the *theorem 1* is completely proved.

Figure 5 demonstrates the validity of solutions (2.30) - we see comprehensive coincidence of the analytical dependences (points) and numerical integration results (lines). Case Fig.5-a corresponds to the first root $r_0^{(1)}$ of the quadratic equation (2.12); case fig.5-b – to the second root $r_0^{(2)}$.

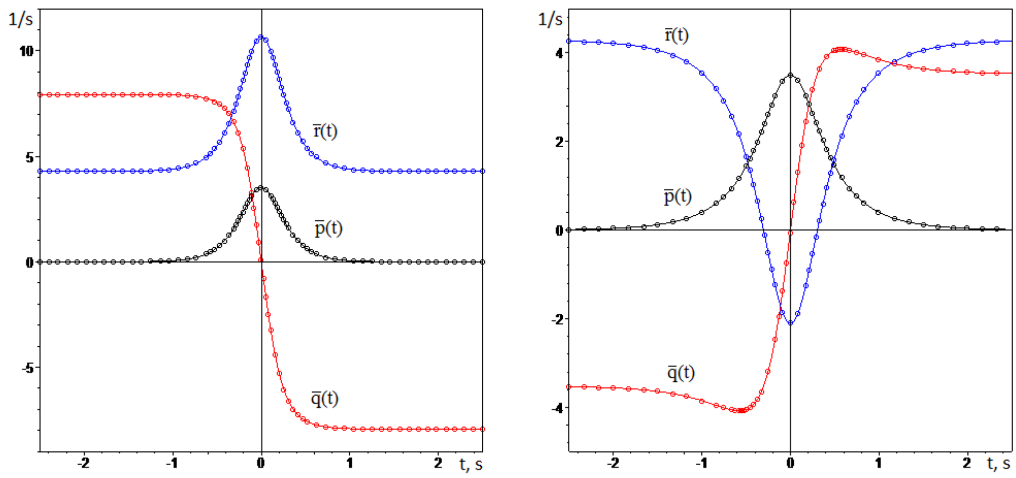

(a) (b)

Fig.5 *The heteroclinic solutions.*

A_2=15; B_2=8; C_2=6; A_1=5; C_1=4; p_0=3.5; $\Delta=30$

a). $r_0=r_0^{(1)}=10.68;\quad \sigma_0^{(1)}=-3.18$ b). $r_0=r_0^{(2)}=-2.10;\quad \sigma_0^{(2)}=9.60$

The solutions (2.30) generalize well known heteroclinic dependencies for the free rigid body, which were used in many scientific works, for example [11, 24].

Task of heteroclinic solutions obtaining in similar formulation was considered in [1, 2, 12 and 16]. In contrast to [1, 12] in this paper the native dynamics of coaxial bodies was investigates without maintaining of constancy of the gyrostatic moment ($h_z=C_1\sigma\neq\text{const}$).

In Ref. [16] heteroclinic solutions were obtained in the Andoyer–Deprit canonical variables on the base of classical procedure [26] for integration of a second order differential equations system (for single degree-of-freedom system), which include following four main steps: 1) the system first integral (energy integral/ Hamiltonian) identification, 2) use of the first integral to reduction of the second order system to the first order system, 3) integration of the first order differential equation in explicit form (in quadrature), 4) inversion of the quadrature and reduction to obtain the single-valued final solution. This procedure was effective applied by prof. Aslanov to obtaining of the coaxial bodies heteroclinic solutions in [16]. With the help of Ref. [16] solutions heteroclinic dependencies for the coaxial bodies angular velocity components also can be written, but in this case shape of solutions will be cumbersome.

On the base of Ref. [16] solutions for the Andoyer–Deprit variables $\left\{\bar{L}=\bar{L}(t),\ \bar{l}=\bar{l}\left(\bar{L}(t)\right)\right\}$ and kinematic expressions (1.3) we can write the heteroclinic dependencies for the angular velocity components $\left\{\bar{p}(t),\bar{q}(t),\bar{r}(t)\right\}$. In this case we get complicated (in comparison with (2.30)) shape of expressions, which include compositions of radicals, exponents, trigonometric functions and inverse trigonometric functions [16]:

$$
\begin{aligned}
A\bar{p}(t)&=\sqrt{I_2^2-\bar{L}^2(t)}\sin\left[\pm\frac{1}{2}\arccos\left(\frac{h-\tilde{a}_1\left(I_2^2-\bar{L}^2(t)\right)-\dfrac{\bar{L}^2(t)}{2C_2}+\dfrac{\Delta\bar{L}(t)}{C_2}}{\tilde{a}_2\left(I_2^2-\bar{L}^2(t)\right)}\right)\right]\\
B\bar{q}(t)&=\sqrt{I_2^2-\bar{L}^2(t)}\cos\left[\pm\frac{1}{2}\arccos\left(\frac{h-\tilde{a}_1\left(I_2^2-\bar{L}^2(t)\right)-\dfrac{\bar{L}^2(t)}{2C_2}+\dfrac{\Delta\bar{L}(t)}{C_2}}{\tilde{a}_2\left(I_2^2-\bar{L}^2(t)\right)}\right)\right]
\end{aligned}
\tag{2.31}
$$

where $h,\ \tilde{a}_1,\ \tilde{a}_2-\text{const}$; structure of the time-dependence $\bar{L}(t)$ [16] is similar to $y(t)$. Reduction of the dependencies (2.31) [16] to the simple form (2.30) by transformations is impossible. In turn, the new solutions (2.30) allow easy writing of dependencies $\left\{\bar{L}=\bar{L}(t),\ \bar{l}=\bar{l}(t),\ \bar{l}=\bar{l}\left(\bar{L}(t)\right)\right\}$:

$$
\begin{aligned}
&\bar{L}(t)=C_2\bar{r}(t)+\bar{\Delta}=C_2y(t)+W\\
&\bar{l}(t)=\arcsin\frac{A\bar{p}(t)}{\sqrt{I_2^2-\bar{L}^2(t)}}=\pm\arcsin\frac{Vy(t)}{\sqrt{I_2^2-\left(C_2y(t)+W\right)^2}}\\
&\bar{l}\left(\bar{L}(t)\right)=\pm\arcsin\frac{V\bar{L}(t)-W}{C_2\sqrt{I_2^2-\bar{L}^2(t)}}
\end{aligned}
\tag{2.32}
$$

where $V=\sqrt{\dfrac{AC_2\left(B-C_2\right)}{\left(A-B\right)}}=\text{const},\quad W=\dfrac{\bar{\Delta}B}{B-C_2}=\text{const}$.

The expressions (2.32) have simple form in comparison with paper [16] results.

In paper [12] important closed-form heteroclinic solutions for gyrostat with the constant gyrostatic moments $\left(h_x,h_y,h_z-\text{const}\right)$ were obtained on the base of Volterra-Wangerin-Wittenburg method. Analytical solutions for the angular velocity components of the body-carrier [12] in this case have cumbersome shape with fractional polynomial functions of hyperbolic tangents (highest power of polynomials equal to 12). Practical use of solutions [12] involves great difficulties at analytical and numerical computations.

Thus, in present paper on the base of Euler dynamical equations (1.2) integration and geometrical analysis of the polhodes disposition in the space of angular velocity components we have obtain the new heteroclinic solutions (2.30). Similar method was applied in [1] to obtaining of solutions for angular velocity components of balanced gyrostat.

3. The motion chaotization analysis

Let us examine possibility of the system motion chaotization with the help of Melnikov method [22] at presence of the perturbation torque (1.6).

The Melnikov function in considered case has the form:

$$M\left(t_0\right)=\int_{-\infty}^{+\infty} f_L\left(\bar{l}\left(t\right),\bar{L}\left(t\right)\right)g_l\left(t+t_0\right)dt \tag{3.1}$$

Take into account (1.3) we can rewrite the integral (3.1):

$$\begin{gathered}M\left(t_0\right)=\int_{-\infty}^{+\infty}\alpha\nu\left(I_2^2-\bar{L}^2\right)\sin\bar{l}\,\cos\bar{l}\,\sin\left(\nu\left(t+t_0\right)\right)dt=\alpha\nu\int_{-\infty}^{+\infty}A\bar{p}(t)B\bar{q}(t)\sin\left(\nu\left(t+t_0\right)\right)dt=\\ =\alpha\nu\int_{-\infty}^{+\infty}A\bar{p}(t)B\bar{q}(t)\left[\sin\left(\nu t\right)\cos\left(\nu t_0\right)+\cos\left(\nu t\right)\sin\left(\nu t_0\right)\right]dt= \\ =\alpha\nu AB\left[\cos\left(\nu t_0\right)J_1+\sin\left(\nu t_0\right)J_2\right]\end{gathered} \tag{3.2}$$

where

$$J_1=\int_{-\infty}^{+\infty}\bar{g}\left(t\right)\sin\left(\nu t\right)dt;\qquad J_2=\int_{-\infty}^{+\infty}\bar{g}\left(t\right)\cos\left(\nu t\right)dt \tag{3.3}$$

$$\bar{g}\left(t\right)=\bar{p}(t)\bar{q}(t)=\pm\sqrt{\frac{C_2\left(B-C_2\right)}{A\left(A-B\right)}}\sqrt{s^2-k^2\left(y\left(t\right)+\Delta\beta\right)^2}\,y\left(t\right),\qquad \Delta=\bar{\Delta}=\text{const} \tag{3.4}$$

The function (3.4) is odd and rapidly damped to zero value (fig.6-a). The first improper integral (3.3), as area of curvilinear figures delineated by even function $g\left(t\right)\sin\left(\nu t\right)$ (fig.6-b), converges to constant *R*. The second improper integral, as area of curvilinear figures delineated by odd function $g\left(t\right)\cos\left(\nu t\right)$ (fig.6-c), is equal to zero:

$$J_1=R=\text{const}\neq 0,\quad J_2=0 \tag{3.5}$$

The result (3.5) also may be obtained by analytical reducing.

The Melnikov functions (3.2) take the cosine form

$$M\left(t_0\right)=\alpha\nu ABR\cos\left(\nu t_0\right) \tag{3.6}$$

Therefore, the Melnikov function has infinite number of simple roots. This proves the fact of the polhode-separatrix-orbit splitting at presence of small harmonical perturbation torques between the coaxial bodies. The splitting of the polhodes-separatrces-orbits implies separation and multiple intersection of stable and unstable manifolds of saddle heteroclinic points. Therefore close to the heteroclinic orbit phase trajectories form very complicated heteroclinic net, which generates the chaotic layer near the separatrix region. The chaotic layer has been illustrated (fig.7, 8) with the help of Poincaré sections $\left(\nu t \bmod 2\pi\right)=0$ in the phase space $\left\{l,L/I_2\right\}$ (the coordinate axes values are dimensionless). Fig.7 contains calculation results for subcritical value $\bar{\Delta}<\Delta^*$ and subcritical topology (fig.2); fig.8 corresponds to critical value $\bar{\Delta}=\Delta^*$ and critical topology (fig.3).

Inside the chaotic layer the phase trajectory can passes through different phase space regions and, therefore, the DSSC performs complicated chaotic evolution with repeated escapes (rotation-oscillation-rotation-…).

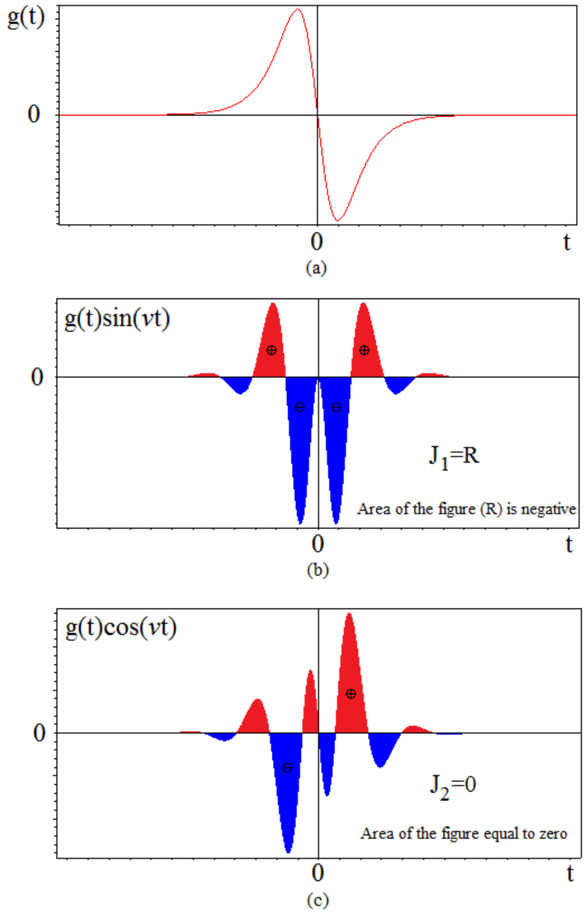

Fig.6

4. Numerical modeling results

In previous section we have proved the fact of the separatrix-polhode splitting and its manifolds intersections on the base of Melnikov's analytical method. This effect led to generation of the heteroclinic net with Smale's horseshoes in the neighborhood of the unperturbed heteroclinic orbit.

In addition to the powerful analytical analysis, it is very important to provide a many-sided numerical investigation of chaotic modes in the system.

First of all, the chaotic layer can be detected with the help of Poincaré sections. The Poincaré section like "stroboscopic photography" demonstrates the system phase space at the time moments with integer period of the harmonic perturbation $\left[(\nu t \bmod 2\pi)=0\right]$. Figures 7 and 8 illustrate the phase portraits with the chaotic layer near the separatrix in the Andoyer–Deprit phase space.

Time-dependencies graphs (fig.9), polhode 3D-curve (fig.10-a) and Poincaré map "stroboscopic"points of the polhode (fig.10-b) also show chaotic nature of the DSSC motion at presence of perturbed torque.

One of the interesting modeling results is the heteroclinic net plotting. We can plot the heteroclinic net as a set of Poincaré map images of the unperturbed separatrix polhode. In the fig. 11 we present six Poincaré-map-forward-iterations (in the forward direction of time $t:0\to+\infty$) of the unperturbed heteroclinic separatrix. In the fig. 12 six Poincaré-map-forward-iterations and six Poincaré-map-back-iterations (in the back direction of time $t:0\to-\infty$) are depicted. As can we see (fig.11), invariant fractal sets (Smale's horseshoes) in neighborhood of the unperturbed separatrix takes places. Intersections of the forward-iterations (red color) and the back-iterations (blue color) led to generation of the heteroclinic net (fig.12).

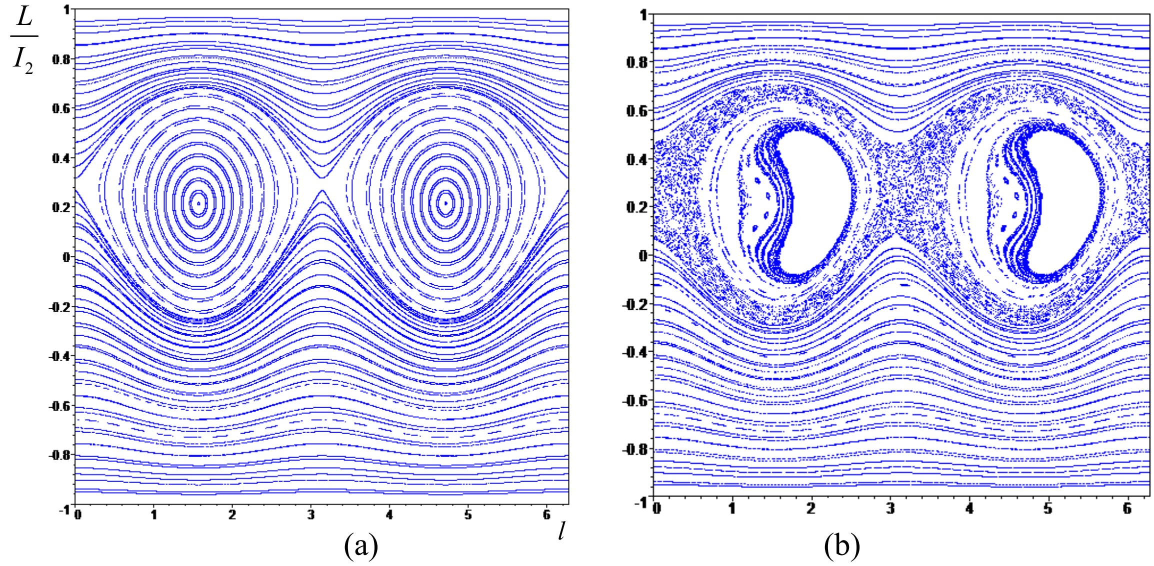

(a) (b)

Fig.7. *Poincaré sections*

$A_2 = 15,\ B_2 = 8,\ C_2 = 6,\ A_1 = 5,\ C_1 = 4;\quad I_2 = 20;\quad \overline{\Delta} = 3:$

a). $\varepsilon = 0$; b). $\varepsilon = 0.05$; $\mu = 0.3$; $\nu = 1.0$

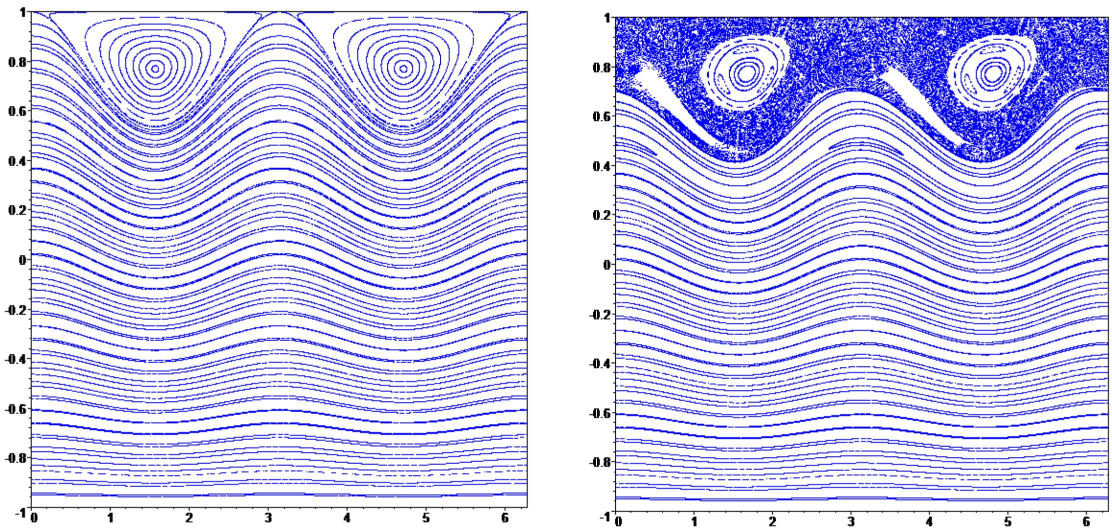

(a) (b)

Fig.8. *Poincaré sections*

$A_2 = 15,\ B_2 = 8,\ C_2 = 6,\ A_1 = 5,\ C_1 = 4;\quad I_2 = 20;\quad \overline{\Delta} = \Delta^* = 10.77$

a). $\varepsilon = 0$; b). $\varepsilon = 0.05$; $\mu = 0.3$; $\nu = 1.0$

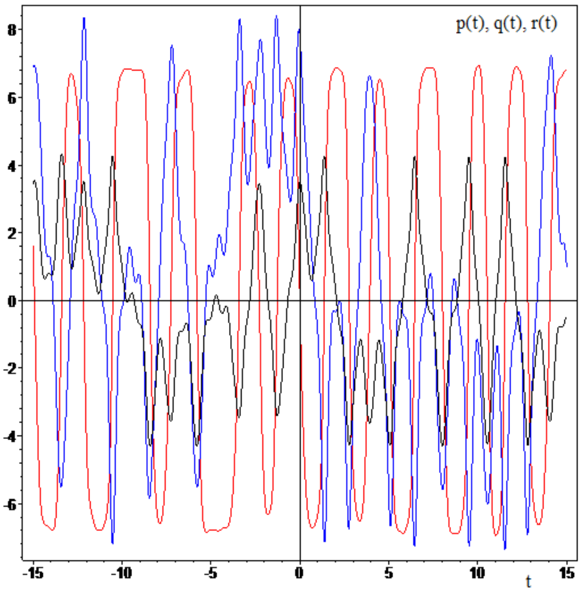

Fig.9. *Time history of the angular velocity component:*
$A = 20;\ \ B = 13;\ \ C = 10;\ \ C_2 = 6;\ \ \Delta = 10;\ \ \nu = 0.1;\ \ \varepsilon = 0.066;$
p(t) – black; q(t) – red; r(t) - blue

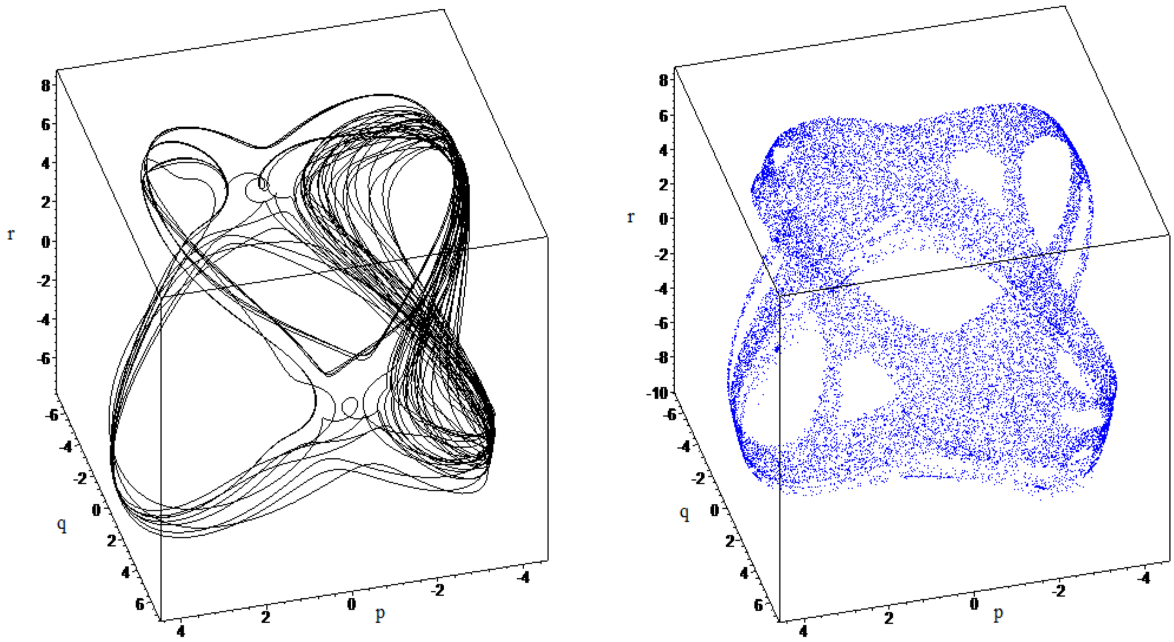

Fig.10. *The perturbed polhode*

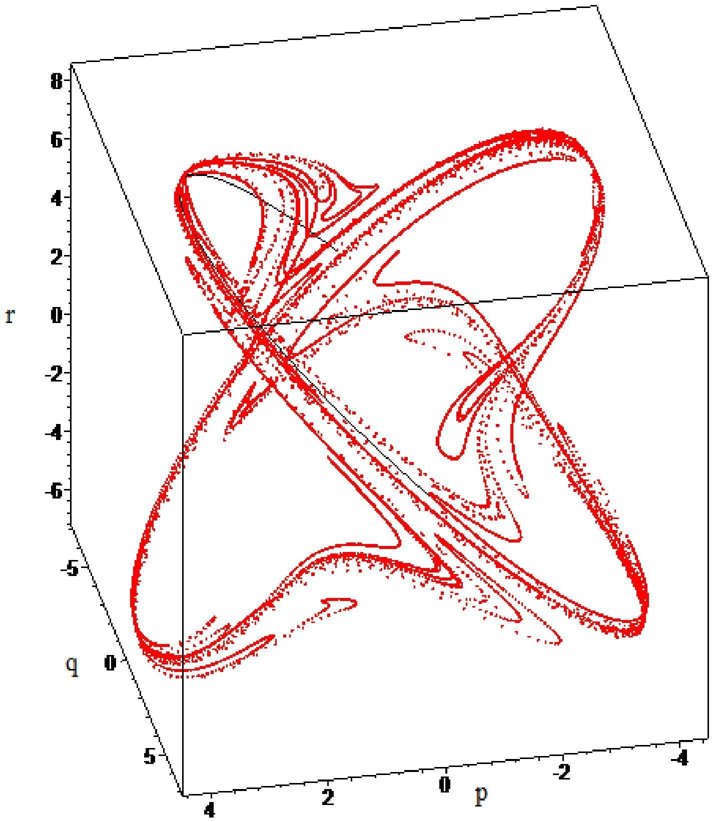

Fig.11. *Poincaré map images of the unperturbed separatrix and Smale's horseshoes initiations*

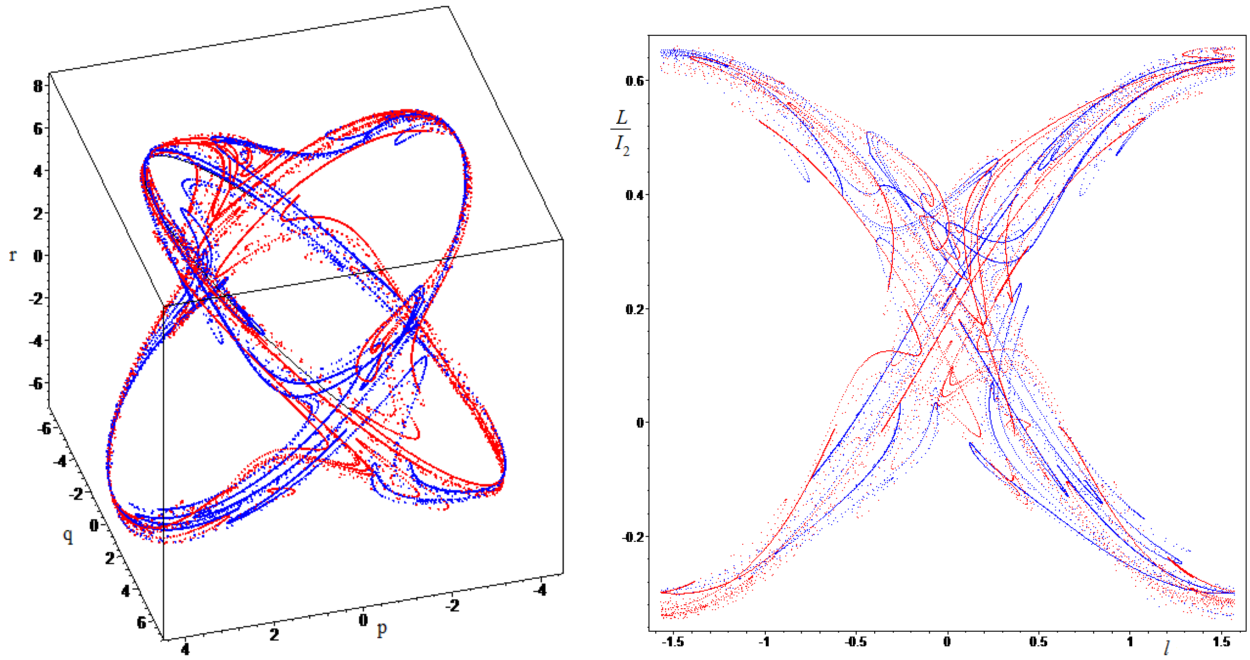

(a) (b)

Fig.12. *Poincaré map images of the unperturbed separatrix and the heteroclinic net*:
a). In the angular velocity components phase space
b). In the Andoyer–Deprit phase space

Conclusion

Heteroclinic dynamics of the free coaxial bodies system and dual-spin spacecraft has been examined. The new analytical solutions for the heteroclinic orbits corresponded to the polhode-separatrix in the space of the angular moment components have been obtained. On the base of these analytical heteroclinic solutions analysis of possibility of the system motion chaotization with the help of Melnikov method has been conducted. The analysis has proved the fact of the polhode-separatrix-orbit splitting at presence of small harmonic perturbation torques of the coaxial bodies internal interaction. The splitting of the polhodes-separatrces-orbits implies separation and multiple intersections of stable and unstable manifolds of saddle heteroclinic points. Therefore close to the heteroclinic orbit phase trajectories form the very complicated heteroclinic net, which generates the chaotic layer near the separatrix region. Inside the chaotic layer phase trajectory can passes through different phase space regions and, therefore, the DSSC performs complicated chaotic evolution with repeated escapes (rotation-oscillation-rotation-…) and the complex tilting motion.

Acknowledgements

This research is supported by the Russian Federation Presidential Program for the Support of Russian Scientists and Leading Scientific Schools (MK-1497.2010.8) and Russian Foundation for Basic Research (RFBR# 11-08-00794-a).

References

1. J. Wittenburg, Dynamics of Systems of Rigid Bodies. Stuttgart: Teubner, 1977.
2. J. Wittenburg, Beitrage zur dynamik von gyrostaten, Accademia Nazional dei Lincei, Quaderno N. 227 (1975) 1–187.
3. H. Andoyer, Cours de Mecanique Celeste, Paris: Gauthier-Villars, 1924.
4. A. Deprit, A free rotation of a rigid body studied in the phase plane, American Journal of Physics 35 (1967) 425 – 428.
5. V.V. Kozlov, Methods of qualitative analysis in the dynamics of a rigid body (in Russian) Gos. Univ., Moscow, 1980. 241 pp.
6. V.V. Kozlov, Integrability and non-integrability in Hamiltonian mechanics. Russian Mathematical Surveys (1983), 38(1):1.
7. E.A. Ivin, Decomposition of variables in task about gyrostat motion. Vestnik MGU (Transactions of Moscow's University). Series: Mathematics and Mechanics. No.3 (1985) Pp. 69-72.
8. A.I. Neishtadt, M.L. Pivovarov, Separatrix crossing in the dynamics of a dual-spin satellite. Journal of Applied Mathematics and Mechanics, Volume 64, Issue 5, 2000, Pages 709-714.
9. C.D. Hall, R.H. Rand, Spinup Dynamics of Axial Dual-Spin Spacecraft, Journal of Guidance, Control, and Dynamics, Vol. 17, No. 1 (1994) 30–37.
10. C.D. Hall, Momentum Transfer Dynamics of a Gyrostat with a Discrete Damper, Journal of Guidance, Control, and Dynamics, Vol. 20, No. 6 (1997) 1072-1075.
11. M. Inarrea, V. Lanchares, Chaos in the reorientation process of a dual-spin spacecraft with time-dependent moments of inertia, Int. J. Bifurcation and Chaos. 10 (2000) 997-1018.
12. J. Kuang, S. Tan, K. Arichandran, A.Y.T. Leung, Chaotic dynamics of an asymmetrical gyrostat, Int. J. Non-Linear Mech. 36 (2001) 1223-1243.

13. A. Guran, Chaotic motion of a Kelvin type gyrostat in a circular orbit, Acta Mech. 98 (1993) 51–61.
14. X. Tong, B. Tabarrok, F. P. J. Rimrott, Chaotic motion of an asymmetric gyrostat in the gravitational field, Int. J. Non-Linear Mech. 30 (1995) 191-203.
15. V.S. Aslanov, Spatial chaotic vibrations when there is a periodic change in the position of the centre of mass of a body in the atmosphere. Journal of Applied Mathematics and Mechanics 73, Issue 2 (2009) 179-187.
16. V.S. Aslanov, A.V. Doroshin, Chaotic dynamics of an unbalanced gyrostat. Journal of Applied Mathematics and Mechanics, Volume 74, Issue 5 (2010) 525-535.
17. V.S. Aslanov, A.V. Doroshin, Two cases of motion of an unbalanced gyrostat, Mechanics of solids, ALLERTON PRESS, INC., Vol. 41, No. 4, (2006). 29-39.
18. A.V. Doroshin, Analysis of attitude motion evolutions of variable mass gyrostats and coaxial rigid bodies system, Int. J. Non-Linear Mech. 45 (2010) 193–205.
19. A.V. Doroshin, Evolution of the precessional motion of unbalanced gyrostats of variable structure. Journal of Applied Mathematics and Mechanics 72, Issue 2 (2008) 269–279.
20. A.V. Doroshin, Modeling of chaotic motion of gyrostats in resistant environment on the base of dynamical systems with strange attractors. Communications in Nonlinear Science and Numerical Simulation, Volume 16, Issue 8 (2011) 3188–3202.
21. A.V. Doroshin, Dual-spin spacecraft motion chaotization in the neighborhood of mode, which stabilized by partial twist // Control in the technical systems. Transactions of the conference UTS-2010. Saint Petersburg, Russia, "Concern CSRI Elektropribor, JSC" (2010) 341-344 (in Russian) http://uts2010.ipu.ru/uts2010/UTS-2010Volume.pdf.
22. V.K. Melnikov, On the stability of the centre for time-periodic perturbations, Trans. Moscow Math. Soc. No.12 (1963) 1-57.
23. S. Wiggins, S.W. Shaw, Chaos and three-dimensional horseshoe in slowly varying oscillators. ASME J. Appl. Mech. 55 (1988) 059-968.
24. P. J. Holmes, J. E. Marsden, Horseshoes and Arnold diffusion for Hamiltonian systems on Lie groups, Indiana Univ. Math. J. 32 (1983) 283-309.
25. H. Poincaré, Les Methods Nouvelles de la Mechanique Celeste. Gautheir-Villars. Paris, 1892.
26. M. Tabor, Chaos and Integrability in Nonlinear Dynamics: An Introduction. Wiley, John & Sons, New York, 1989.
27. B. Chirikov, A universal instability of many dimensionaloscillator system. Phys. Reports, 52, 273 (1979).
28. J. M. Greene, A method for determining a stochastic transition. J. Math. Phys., 20, 1183 (1979).
29. I. S. Gradshteyn, I. M. Ryzhik, Table of Integrals, Series and Products, Academic Press, San Diego, 1980.